Hydrogen in jellium: First-principles pair interactions

S. A. Bonev and N. W. Ashcroft

Laboratory of Atomic and Solid State Physics and Cornell Center for Materials Research, Cornell University,
Ithaca, New York 14853-2501

Ground-state pair potentials between protons immersed in jellium (interacting electrons plus a compensating background) and at densities corresponding to the range $1 < r_s < 4$ are calculated using first-principles density functional theory methods. While the results obtained for immersing a single H atom in an electron gas agree with previous calculations, it is discovered that molecular-type short-range binding becomes unstable at surprisingly low density (at about $r_s = 3.2$), and that at even lower density there is a bistability between a weakly bound molecule and an unpaired state. This behavior is a result of the possible pairing of hydrogen and itinerant jellium electrons with little electrostatic penalty, a consequence of the positive background filling the entire volume V. Another important finding is a density range ($1.5 < r_s < 2$) where the pair potentials are insufficiently strong to bind the protons, suggesting the possibility of inducing hydrogen into a state of low-temperature quantum fluid at a critical density.

I. INTRODUCTION

Dense hydrogen has proven to be an extremely intriguing and subtle quantum system. It has long been predicted to undergo a sequence of diatomic orderings and transitions as density is increased under the application of external pressure. At high enough pressure, a fully dissociated metallic state, first considered by Wigner and Huntington,[1] is expected. Because it is a fundamental system, the behavior of hydrogen at high pressures and densities has attracted considerable attention,[2–4] and it remains a matter of active theoretical and experimental debate.

Ironically, the very simplicity of the hydrogen atom, having but a single electron, also contributes to the complexity of its dense state. Because of the lack of closed inner shells of core electrons, and being one electron short of a closed outer shell, hydrogen is very different from other light elements (despite its traditional presence in group I of the periodic table). Its molecular or paired structure survives to surprisingly high densities in the condensed phase; and diatomic pairing of hydrogen at metallic densities is also a manifestation of the strong, nonlinear electron-ion interactions which lead, via exchange, to the accumulation of extra electronic charge between the atoms forming a given pair. Consequently, standard perturbation approaches, such as linear- and higher-order response theory, that are generally satisfactory for other metals with closed inner shells, are insufficient for hydrogen. It is clear that proper inclusion of the electron-proton interaction, and the resulting effective state dependent pair and higher-order interactions are keys to understanding the properties of dense hydrogen, the hydrogen plasma, and metal hydrides. Naturally, the study of a simplified system, where the protons, with the requisite compensating electrons, are embedded in a previously formed homogeneous electron gas with neutralizing rigid background (the standard jellium problem), has been a route yielding considerable insight.[5–15]

We arrive at the system discussed in this paper by considering a specific proton pair, with associated electronic component, to be viewed as being excerpted from $N/2$ such pairs.

The remaining outer $(N/2 - 1)$ pairs are then replaced by a system where the discrete proton charge is transformed into a uniform background. For what follows it is important to remark immediately that the uniform (positive) background actually fills the *entire* volume V. As will be seen, the physical consequences of this are not trivial for the remaining proton pair, which now resides in an otherwise standard electron gas. In the present model the effect of compression is realized as follows; in the original problem, N protons and N electrons are densified in a uniform manner. Here densification alters the penetrating uniform background and the compensating system of electrons. Together they have an influence on the selected molecule and in this way the effect of compression in dense hydrogen is being mimicked by the systematic densification of an outer electron gas on an inner molecule.

In this paper we therefore wish to examine the hydrogen-hydrogen (or proton-proton) interactions in the ground state of such an electron gas, and at densities corresponding to the range $1 < r_s < 4$, where $4\pi/3 r_s^3 a_0^3 = N/V$ for N electrons in a volume V, where the average electronic density of solid hydrogen at 1 atmosphere corresponds to $r_s = 3.13$, and where the local value of r_s at the proton in the hydrogen atom is 0.89. Most of the previous studies of the H-H interactions in jellium have concentrated either on the short-range or on the long-range interactions. Nørskov[5] studied the former by solving the Dyson equation for the change in the Green's function of the electron gas associated with the H impurities, by projecting it onto a finite localized basis set; and later he addressed the same problem with effective medium theory.[6] Ferraz *et al.*[7] proposed a Heitler-London method, but with Thomas-Fermi screened interactions, to study the hydrogen metallization. These approaches are based on the assumption of H_2-like interactions and/or charge densities, and naturally fail for larger interproton distances and higher densities (where there are no electron states bound to the protons). Christensen *et al.*[8] performed self-consistent calculations within the local-density approximation (LDA) at $r_s = 2.95$. They situated H_2 molecules on a fcc lattice but with one extra electron per unit cell and their results only extend to H-H separations of 3.0 a.u. At larger separations, the single

extra electron cannot be representative of jellium because of the eventual formation of H^--like ions, as we will show later. Perrot and Rasolt[9] obtained long-range Friedel oscillations in the effective pair potential $\Phi^{(2)}(r)$ by expanding the kinetic energy functional to fourth order and superimposing the charge densities induced from individual ions. Later Perrot[10] interpolated the long-range pair potential based on a new formulation of the kinetic energy functional and the short-range potential from effective-medium H_2-like interaction.

These approaches are valuable but have the shortcoming that they are not applicable to all densities and all separations; they require different sets of approximations for the short- and long-range interactions and the interpolation between these two limits is not straightforward. In addition, although they agree qualitatively, they give quantitatively different results. Zong and Ceperley[11] calculated $\Phi^{(2)}(r)$ at $r_s=3.93$ and 2.07 using the path integral Monte Carlo (PIMC) method, which does not require specification of wave functions and which can be applied in principle to an extended system (although the results in Ref. 11 are for proton-proton separations up to 3 a.u.). However, the PIMC is applicable only for finite temperatures, and Zong and Ceperley used $T=1/16$ Hartree ($\equiv 20\,000$ K), which is actually quite large compared to our energy scales, as we will see later. Accordingly, to address these points we report below large scale ground state *ab initio* band structure calculations of the H-H interactions in jellium designed to treat a substantial density range and quite extended separations. As will be seen, the pair potential curves that we obtain have numerical errors in the relative energies only of the order of 10^{-3} eV. The results are also valid both in the local spin density approximation (LSDA) and within the generalized gradient approximation (GGA). Since in density functional theory we need not assume any charge density *a priori*, all ranges are treated on the same footing in our calculations. Thus, we have been able to compare the short- and long-range energies and unveil a very surprising feature. At low density ($r_s > 3$), the embedded hydrogen molecule, which is otherwise little affected by the jellium at around its equilibrium dimer distance, actually dissociates at interproton distances $2a_0 < R < 3a_0$, with very small dissociation barrier (as low as 0.08 eV at $r_s=3.2$), and to an unpaired state with lower energy. We will show that the presence of itinerant electrons, ensured by the uniform positive background, plays an essential role here. Note that in the unpaired state mentioned above, the protons may be actually bound by the long-range oscillating part of the pair potentials; they are unpaired in the sense that they do not form molecules. However, we have also found that in the density range corresponding to (approximately) $1.5 < r_s < 2$, the pair potentials are insufficiently strong to bind the protons, suggesting the possibility that in the presence of proton dynamics solid hydrogen can undergo a pressure melting at a critical density, which was first proposed by Brovman *et al.*,[16] and later investigated by Ceperley[17] using quantum Monte Carlo; it also has been predicted with a different argument by Ashcroft.[18]

The remainder of the paper is organized as follows. The computational method is described in Sec. II, the results are

TABLE I. Summary of parameters used for the calculations of the p-p pair potential plots; a is the lattice constant of the cubic superlattice and N is the number of electrons per unit cell.

r_s	a (a.u.)	N	k-point mesh
1.3	16.8	512	$6\times6\times6$
2.0	20.5	256	$4\times4\times4$
2.65	21.5	124	$4\times4\times4$
3.2	26.0	128	$4\times4\times4$
3.93	25.3	64	$4\times4\times4$

presented and discussed in Sec. III, and conclusions are given in Sec. IV.

II. COMPUTATIONAL METHOD

The system considered is actually a periodic array of "large" cubic supercells, each containing N electrons, 1 or 2 protons, and the requisite neutralizing rigid background. The role of the background is limited to canceling the divergent $\mathbf{k}=0$ term of the electrostatic potential. The electronic structure problem for this system is treated using standard density functional methods, where the Kohn-Sham equations[19,20] are solved self-consistently by expanding the electronic states in a plane wave basis. We have carried out the computations with both the Vienna *ab initio* simulations package (VASP), and Abinit algorithms. For a description of the plane-wave method and the concepts employed in these algorithms we refer the reader to the papers by Kresse *et al.*[21] and Payne *et al.*[22]

To determine the proton-proton pair potential, the ground-state energy of the system is computed at a series of fixed interproton separations. Since each cubic cell is intended to represent an infinite system, the convergence of all results with size is essential and has been ensured; and we have also verified that the results do not differ when varying the orientation of the proton pair relative to the cell geometry. We have used Monkhorst-Pack type $\mathbf{k}$-point meshes[23]; because of the large unit cells, typical meshes, resulting in convergence of less than 1 meV, are $6\times6\times6$ at $r_s=1.3$ ($N=512$), and $4\times4\times4$ at $r_s=3.2$ ($N=128$). Jellium, being a perfect Fermi liquid at high enough densities, has an occupation function that jumps from 1 to 0 at the Fermi level and this usually causes serious convergence problems; these have been treated using the smearing method of Methfessel and Paxton[24] (with a typical smearing temperature, $\sigma=0.2$ eV). The resulting maximum errors in the total energies in terms of the introduced entropy are of the order of 10 meV per unit cell (100 to 500 electrons), and errors in the energy *differences* are naturally much smaller. A summary of the parameters used for the pair potential plots is given in Table I.

The plots of the pair potential given in the next section are from computations with VASP, within the LSDA [using the Ceperley and Alder[25] (CA) exchange-correlation parametrized by Perdew and Zunger[26]], and with 7.35 Hartree energy cutoff ultrasoft pseudopotential supplied by Kresse and Hafner.[27,28] However, we have also confirmed the features (i) using corrections originating with the GGA [Perdew-Wang

91 (Refs. 29,30)]; (ii) with norm-conserving pseudopotentials supplied by Teter,[31] with core radii as small as 0.1 a.u. (with plane wave cutoffs up to 80 Hartree) and using Abinit (LSDA, Teter parametrization of CA); and (iii) with a bare Coulomb potential $-1/r$ and energy cutoff as high as 200 Hartree. We find that the choice of pseudopotential (or $-1/r$ potential) and exchange-correlation has practically no effect on the energy differences (it is certainly not greater than our numerical errors).

Although we are mainly interested in the energy differences, we have also established the pair potentials on an absolute scale. We define the energy E_b as

$$E_b(r_s,R)=E(Ne,2p;R)-E[(N-2)e]-2E(H),\quad(1)$$

where $E(Ne,2p;R)$ is the energy per cell, where each cell contains N electrons and 2 protons separated by a distance R, $E[(N-2)e]$ is the energy of a uniform gas with $N-2$ electrons in a cell, and $E(H)$ is the LSDA energy of a hydrogen atom in vacuum. All of these quantities are calculated directly with the *ab initio* algorithms. The physical meaning of E_b is that it is the energy of embedding a pair of hydrogen atoms in the background neutralized electron gas. The quantity $\varepsilon_b(r_s)=1/2E_b(Ne,2p;R\rightarrow\infty)$, which is the energy of embedding a single H atom, can be compared with earlier work,[5,12–15] and gives additional physical insight into the problem.

When adding a hydrogen pair to each cell, the average density changes from $(N-2)/V$ to N/V. It might seem that the energies $E(Ne,2p;R)$ and $E[(N-2)e]$ are now defined at two different densities, and in principle such an ambiguity could then pose a problem for the intended physical interpretation of $E_b(r_s,R)$, because the convergence of $(N-2)/V$ and N/V when the cells are enlarged is also accompanied by the equally fast ($\sim N$) increase of $E(Ne,2p;R)$ and $E[(N-2)e]$. But in fact this difficulty can easily be avoided through the realization that the induced charge around a proton is always unity, and that the long-range oscillations in the density must fade away as $1/R^3$. Therefore, we can always make the supercells large enough that the electron charge at their borders is almost uniform at a density $(N-2)/V$. Under such conditions, each cubic cell indeed represents an infinite system and both $E(Ne,2p;R)$ and $E[(N-2)e]$ are defined at the same density, namely,[32] $(N-2)/V$. The amplitudes of the oscillations of the pair potential at separations close to half the cell side are now an estimate for the errors in the calculation of the energy E_b that are related to the finite system size.

The accuracy of the total energy calculations, and hence E_b, depend also on the quality of the pseudopotentials used. As required by the cusp theorem, the induced charge around the protons contracts when the density is increased. The electrons from the jellium, which now have higher kinetic energy (kinetic energy of uniform gas goes as $1/r_s^2$), can more easily penetrate in the core region. It is obvious that the potential in the immediate vicinity of the protons becomes more important and pseudopotentials designed to produced correct energies at low densities may fail to do so at higher densities. We must emphasize here that the energy *differences* are still little
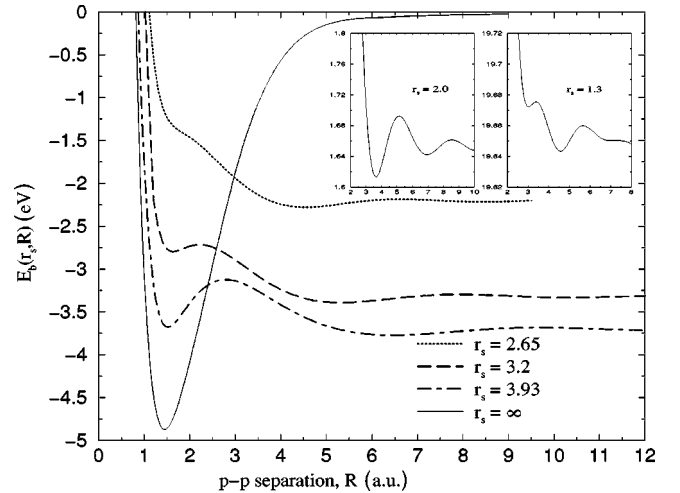

FIG. 1. Pair potentials of H atoms in vacuum and embedded in a background neutralized jellium at selected densities close to the free electron densities found in Na ($r_s=3.93$), Li (3.25), Mg (2.65), and Al (2.07); also the average electronic densities of solid H_2 at 1 atmosphere and at the point of transition to a monoatomic solid correspond to $r_s=3.13$ and 1.3, respectively. $E_b(r_s,R)$ is the energy of bringing two H atoms initially in vacuum and at infinite separation into the electron gas and at separation R.

affected because the bond distances increase with density, so while the short-range effects around the protons become more important for the total energy, the long-range effects become more relevant for the energy differences. To ascertain if the calculations of E_b are independent of the choice of pseudopotential, we have computed the quantity $E(Ne,1p)-E(H)$ at $r_s=1.3$ with different pseudopotentials and also with a $-1/r$ potential with cut off 500 Hartree. We find no noticeable differences when choosing pseudopotentials with smaller core radii.

III. RESULTS AND DISCUSSION

The proton-proton (p-p) pair potential curves at selected densities are shown in Fig. 1, and a summary of their characteristics is listed in Table II. A comparison of our results for the energy of immersing a single hydrogen impurity in jellium ε_b with the previous results of several different groups,[5,13–15] given in Fig. 2, shows very good agreement. The general observation is that ε_b increases with decreasing r_s in the metallic range ($r_s<6$), and eventually becomes positive at about $r_s=2.1$. At lower densities, it is expected to start increasing (slowly) again, and to approach -0.75 eV, the binding energy of an H^- ion, when the chemical potential vanishes. Compared to the free atom, there is a substantial accumulation of extra charge around a hydrogen atom embedded in the electron gas with uniform background (see Fig. 3). The state is paramagnetic at all densities (and p-p separations) indicating pairing between the hydrogen and/or jellium electrons. Similar results for the electron density and magnetic moment of a single hydrogen impurity in jellium have been reported by other authors.[5,13–15] It has been suggested[5,14] that as a basis for the physical understanding of this state a screened H^- ion should be considered. The seem-

TABLE II. Summary of characteristics of the p-p pair potentials: d is the the equilibrium separation and ΔE is the dissociation barrier of the H_2-like short-range interaction; $\Delta E_b = E_b(r_s,d) - E_b(r_s,\infty)$ is the binding energy of a hydrogen molecule in jellium; ε_b is the energy of immersing a single hydrogen atom in jellium; R_m is the separation at which the molecular dissociation barrier has a maximum; R_0 is the first minimum in the long-range oscillating pair potential, and ΔR is its period; k_F is the Fermi wave vector. Lengths are in atomic units, energies in eV. Error bars in the last digit are given in parentheses and are related mostly to the finite cell size and to the introduced entropy due to the smearing of the Fermi surface. All results here are from LSDA calculations with a 7.35 Hartree cutoff ultrasoft pseudopotential.

r_s	d	ΔE	ΔE_b	ε_b	R_m	R_0	ΔR	π/k_F
1.3				9.8(1)		3.01(5)	2.2(1)	2.13
2.0				0.83(2)		3.64(2)	3.3(2)	3.27
2.65				−1.11(1)		4.55(5)	4.0(2)	4.34
3.2	1.63(1)	0.081(3)	0.52(1)	−1.665(5)	2.22(1)	5.30(5)	5.2(1)	5.24
3.93	1.52(1)	0.552(3)	0.02(2)	−1.85(1)	2.79(6)	6.45(10)	6.46(10)	6.43
∞	1.445(5)	4.872(1)	−4.872(1)	0	∞			

ing contradiction between a shallow (screened) H^--like bound state and induced density even more contracted than that of free hydrogen has been justified[5] by the argument that the bound H^- electrons are being screened out primarily by the long-wavelength jellium electrons.

At $r_s > 3$ we find a well defined hydrogen molecule with a dissociation barrier and with an equilibrium bond length somewhat larger than but close to that of the molecule in vacuum; it also displays a similar electron density around the protons (see Fig. 3). The interaction at about the equilibrium distance is H_2-like in the sense that it can be explained in terms of the usual H_2 binding plus perturbative screening from the jellium electrons. However, the dissociation barrier is only 0.08 eV at $r_s = 3.2$, which is less than the zero point vibrational energy of the protons, and it disappears completely at higher densities. Even at $r_s > 3$, the unpaired state has energy close to or lower than the molecule (the isolated

H_2 molecule behavior is of course recovered at very large r_s). This behavior is initially unexpected (though explicable — see below) considering that the density corresponding to $r_s = 3$ is only about 2.6% of the density at the proton in the hydrogen atom (though for other s-p valent metals it is quite high). It cannot be explained in terms of perturbed H_2-like interactions, and this is why methods based on this assumption predict the molecule to remain stable up to densities corresponding to $r_s = 2$ and lower.[6,7,10] We have plotted results for the binding energy of a molecule in jellium from Refs. 6 and 10 in Fig. 4. It shows that, unlike the findings of the present calculations, perturbative methods give the binding energy to be linearly proportional to the density and remain negative up to density corresponding to almost $r_s = 2$.

The reason behind the large differences between the p-p pair potentials in vacuum and in a background-neutralized
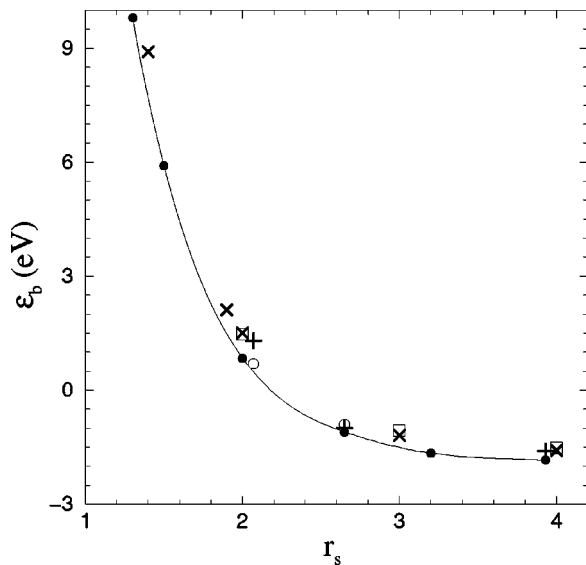

FIG. 2. Energy of embedding a single H atom in jellium as a function of the density parameter r_s; ($\bullet$) present work, ($+$) from Ref. 5, ($\square$) from Ref. 13, (x) from Ref. 14, and ($\circ$) from Ref. 15. The line is a spline interpolation and is only a guide to the eye.
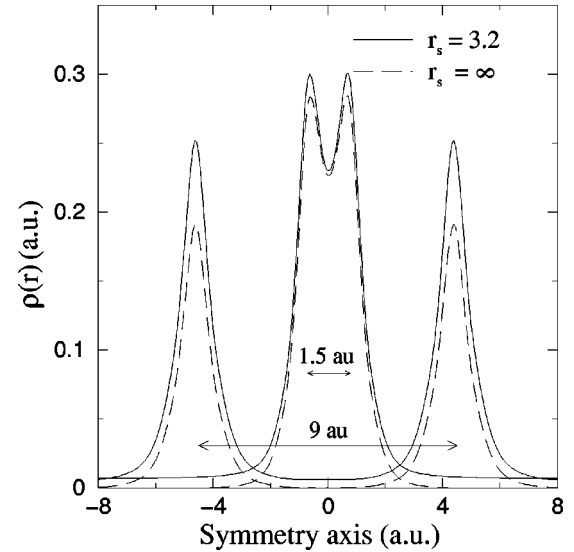

FIG. 3. Electronic densities at p-p separations 1.5 a.u. (molecular state) and 9 a.u. (unpaired state) in vacuum and in an electron gas. The lack of cusps at the proton positions is traced to the use of pseudopotentials. The integrated densities, $r^2\rho(r)$, differ little from calculations with a bare Coulomb potential.
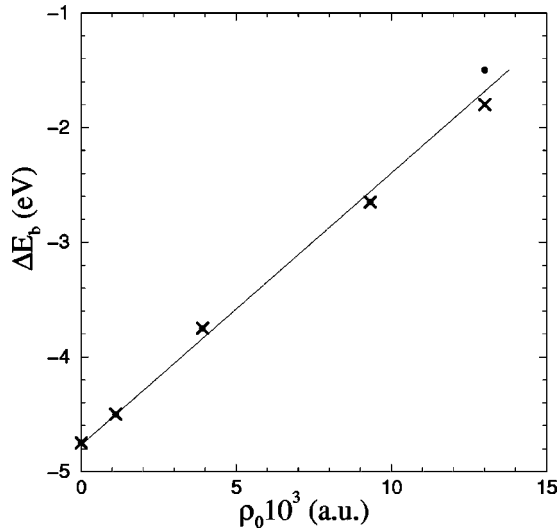
FIG. 4. Binding energy of a H_2 molecule (the energy of 2 H atoms at separation $R \sim 1.5$ diminished by the energy of 2 H atoms at $R = \infty$) as a function of density ($\bullet$) from Ref. 6 and (x) from Ref. 10.

electron gas of relatively low density is clearly related to the pile up of extra charge around the protons in jellium at large separations, illustrated in Fig. 3. A look at the corresponding band structure for the supercell system gives an insight into what is happening. In Fig. 5, we have shown the lowest 8 bands for 2 protons and 128 electrons at different proton separations R and at $r_s = 3.2$ (the molecular band at $R = 1.6$ lies out of the picture to the bottom). First, we observe that there is a flat band that is moving up when the p-p distance is increased. It corresponds to the bonding, singlet state.
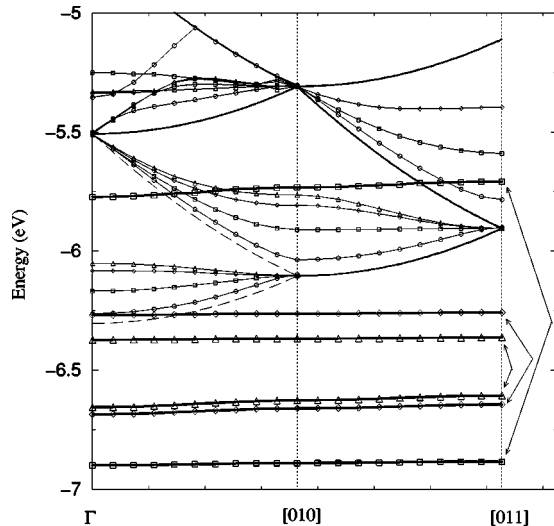

FIG. 5. Band structures at a density corresponding to $r_s = 3.2$ and at 4 different H-H separations ($\bigcirc$) $R = 1.6$, ($\square$) $R = 5.0$, ($\diamond$) $R = 9.0$, and ($\triangle$) $R = 12.0$. The highlighted flat bands correspond to singlet lower) and triplet (upper) H_2 states. The Fermi level is at -1.46 eV and the molecular band for $R = 1.6$ at -11.27 eV. The dashed lines are free electron bands, and the solid lines with no symbols indicate bands which remain the same at *all* p-p separations *and* coincide with the free electron bands.

Then, there are bands that coincide with the free electron bands and remain unchanged, and other bands that are only slightly shifted upward when the protons are moved apart. These bands, even when flat in certain (or in all) directions, correspond to itinerant jellium electrons, and their exact structure can be explained with an impurity induced resonant state, which is not relevant here and will be discussed in a future paper.[33] Finally, and more interestingly, there is another flat band, which appears and moves down for larger p-p separations. This corresponds to a hybridized, triplet, antibonding state, which piles charge over the protons. When the hydrogen atoms are moved apart, the singlet state, which accumulates charge between the protons, causes a depletion of charge at their position. In this way, the electrostatic penalty associated with occupying the triplet state, when the singlet level is already occupied, decreases. When the energy of this state falls below the chemical potential, it becomes occupied by the jellium electrons, thus breaking the molecular bond.[34] Accordingly, the size of the dissociation barrier decreases with density increase and eventually disappears when the energy of the triplet state becomes equal to the chemical potential at p-p separation of about 1.6 a.u.

The energy ε_b, on the other hand, depends on where the singlet and triplet levels merge, and on the influence of the resulting state on the other bands. The former is determined primarily by the average exchange-correlation potential, and decreases with density increase, while the merger of the bonding and antibonding states represents doubly occupied H^- ions, which act as cores that push the other bands upward.[35] Therefore, in this band structure picture, the energy for immersing an H atom in jellium can be understood in terms of the competition between the exchange correlation and kinetic energies.

We also propose here a picture in real space, which can be used to understand the pair potential curves and the induced density around the embedded hydrogen atoms. The binding of the hydrogen molecule (4.7 eV) is largely realized by the exchange-driven singlet pairing of the localized two hydrogen electrons. The result of the pairing is an accumulation of charge between the two protons where the attractive field is stronger. It can also be said that there are two electrons in the field of each proton. The binding of the free H^- ion (also with two electrons around the proton) on the other hand is only 0.75 eV because the ion is not neutral. The fact that in jellium the unpaired state has an energy similar to the H_2 molecule suggests a formation of electron pairs around each proton with little electrostatic penalty. The situation differs from that in vacuum in that the extra electron in the vicinity of the hydrogen atom is now provided by the electron gas. If one were to solve the problem of the embedded hydrogen atom in spherical coordinates, the positive charge inside a sphere of radius r_s and centered at the proton is 2 a.u. The physical picture then resembles a neutral "atom" with one point charge, one smeared positive charge, and two electrons.

The simplest analytical model to describe this situation is a spherical cell model (SCM), acknowledging the charged background and with Hamiltonian

$$\hat{H} = -\frac{\nabla_1^2}{2} - \frac{\nabla_2^2}{2} + \hat{V}(\mathbf{r}_1) + \hat{V}(\mathbf{r}_2) + \frac{1}{r_{12}}, \quad (2)$$

where

$$V(\mathbf{r}) = -\frac{1}{r} + \frac{r^2}{2r_s^3} - \frac{3}{2r_s}, \quad (3)$$

defined for $r < r_s$, is the potential arising from the positive point charge at $r = 0$ and the uniform positive background inside the sphere of radius r_s. As noted earlier, the potential arising from the background is an effective representation of the electrostatic interaction between the electrons inside the cell and the rest of the system.[36] We can further simplify matters if we first treat the electron-electron interaction $1/r_{12}$ as a perturbation and write the two-electron wave function as $\psi(\mathbf{r}_1, \mathbf{r}_2) = \psi(\mathbf{r}_1)\psi(\mathbf{r}_2)$, but also introduce an effective coupling Z as a variational parameter. We can then find $\psi(\mathbf{r})$ as a function of Z from the auxiliary single-particle Schrödinger equation

$$\left\{ -\frac{\nabla^2}{2} + ZV(\mathbf{r}) \right\} \psi(\mathbf{r}) = E_0 \psi(\mathbf{r}). \quad (4)$$

The physical basis of this model is linked to the assumption that the overlap between the wave functions of the electrons inside and outside the cell, which can be measured by $\frac{4}{3}\pi r_s^3 |\psi(r = r_s)|^2$, is negligible, which is a good approximation *only* at low density and when bound electron states exist. To account for the effects of the overlap, we introduce a band-energy correction to E_0 in terms of an effective mass, $m^* = m/\alpha$, namely,

$$E_{bs} = 2\sum_{\mathbf{k}} \frac{\alpha k^2}{2} = \alpha \frac{3}{10} \left(\frac{9\pi}{4} \right)^{2/3} \frac{1}{r_s^2}. \quad (5)$$

We then minimize the variational energy

$$E = \langle \psi(\mathbf{r}_1, \mathbf{r}_2) | \hat{H} | \psi(\mathbf{r}_1, \mathbf{r}_2) \rangle + E_{bs}, \quad (6)$$

where $\hat{H}$ is given by Eq. (2). Here E is minimized with respect to Z, which enters the equation through both ψ and E_{bs}, and Eq. (4) is solved subject to the boundary condition $d\psi/dr|_{r_s} = 0$. The details of the calculation (which has relevance beyond this particular problem) and a justification of the boundary conditions are given in the Appendix. A comparison between the induced density obtained from this model and from the *ab initio* calculations is given in Fig. 6. Considering that the SCM almost completely ignores the quantum nature of the surrounding medium, the agreement is quite satisfactory at densities where there are bound electron states (in the actual system).[37] At higher densities, where there are no bound states and the screening lengths[38] are larger than r_s, there is little physical justification for a determination of the induced density by minimizing the energy of a Schrödinger equation defined *only* inside a sphere of radius r_s, and the model naturally fails. The point that the SCM illustrates is that the presence of itinerant jellium electrons is *crucial* for the shape of the pair potentials at metallic
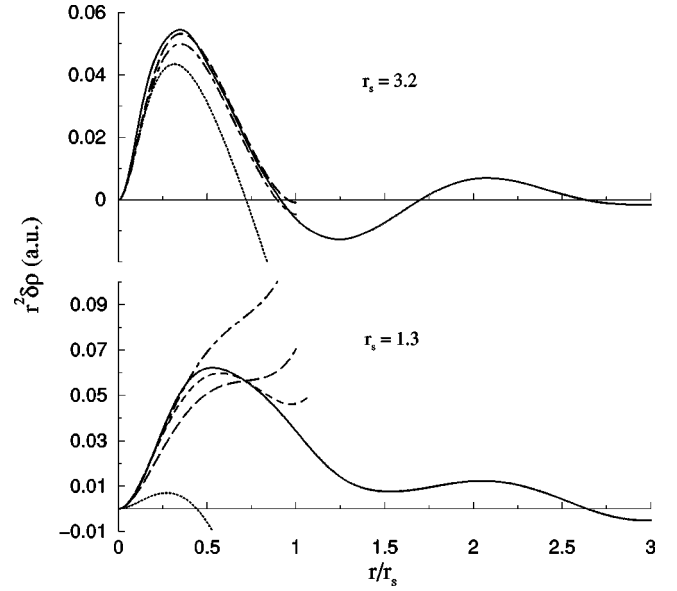

FIG. 6. Integrated induced charge density at $r_s = 3.2$ and 1.3 from (——) *ab initio* calculations, (······) H$^-$ ion, (– · – · –) the SCM, and (— — —) the SCM but with charge normalized to give the *ab initio* charge inside a sphere with radius r_s. The results from the SCM at $r_s = 1.3$ with $Z = 1$ and wave functions normalized inside r_{max} and boundary condition imposed at r_{max}, where r_{max} is such that the *ab initio* charge inside a sphere of radius r_{max} is 2 is also given (- - -).

densities ($r_s > 2$). A hydrogen impurity in a metal can indeed be regarded as a "jellium hydride" state, which is a consequence of the fact that the positive (background) charge fills the entire space. Therefore, results from such jellium models cannot be *directly* translated to *pure* solid hydrogen (in a nonplasma state) where there is but a unit charge associated with each proton.

Structural trends within simple metals can often be accounted for by the form of the (Friedel) oscillating interatomic pair potentials. At very high density, when the oscillations diminish, the structure is determined by the repulsive short-range potentials when they appear at separations larger than twice the Wigner-Seitz radius. What is unique about hydrogen, is that (i) it has small mass and charge, meaning that the magnitude of the oscillations in the pair potentials can become smaller than the energy associated with the zero point motion of the protons at relatively low density compared to other metals and (ii) as noted it does not have inner-shell electrons, as a result of which the repulsive short-range potential is more "contracted" around the protons. We have found that there is a density region ($1.5 < r_s < 2$) where the oscillating *p-p* pair potential is insufficiently strong to bind the protons,[39] and the repulsive short-range potential appears at separations less than $2r_s$ (see inset in Fig. 1). This observation confirms previous predictions of such a state,[16–18] though at a different density. Its physical implications can be far-reaching, namely, that it is possible, by application of pressure, to bring hydrogen to a state of a low-temperature quantum fluid. Notice that at these densities there are no bound states around the protons [the value of r_s at which the Yukawa potential $\exp(-k_{TF}r)/r$ just fails to have a bound

state is 2.4], so the results from the jellium model actually do have relevance to hydrogen plasma. The difference between the two systems is that, at the same average density, the plasma electrons will have larger effective mass than the jellium electrons because of the presence of point positive charges in this system, rather than a uniform background. An exact correspondence between jellium and the hydrogen plasma can be found by comparing the density dependence of the effective mass obtained from the two models, but it is clear that results from the jellium model correspond to those of the hydrogen plasma at higher average density.

IV. CONCLUSION

We have elucidated the evolution with density of proton-proton interactions in jellium. Our results for the energy and induced density of a single hydrogen impurity in an electron gas agree well with previous results. However, when embedded in jellium, the H_2 molecule becomes unstable at much lower density than previously thought. The origin of this behavior, which previous approximate methods have not fully included, is the presence of itinerant jellium electrons, which tend to bind with the hydrogen electrons in competition with the molecular binding, and for which, to repeat, the uniform positive background plays a central role. Therefore, we have concluded that the jellium model cannot be applied directly to study *intramolecular* H-H interactions in pure dense hydrogen. However, the results from this model are especially relevant for interactions between hydrogen impurities in systems with (nearly) free electrons. It is an interesting experimental question whether the bistability between the paired and unpaired states which we find at $r_s > 3.2$ can actually be observed for H impurities in metals or in dense hydrogen supplied with donor impurities. The jellium model is an even more ''realistic'' system in 2D, where it can be mimicked in the inversion region of semiconductors. The main features of the pair potentials should remain similar there, but because of the stronger molecular binding in 2D, the 3D behavior will translate to higher density in 2D.

Finally, we find a range of densities, corresponding to (approximately) $1.5 < r_s < 2$, where the H-H pair potential is insufficiently strong to bind the protons, which suggests the intriguing possibility that hydrogen can be liquified in its ground state simply by systematic application of pressure. Whether this is actually possible, depends on how exactly the jellium system in the density range between $r_s = 1.5$ and 2 maps on the real hydrogen system.[17] It is clear that the effective mass associated with the extremely inhomogeneous electronic distribution in an N-proton system will be much larger than in a jellium model with equal average density.

APPENDIX

With the approximation $\psi(\mathbf{r}_1, \mathbf{r}_2) = \psi(\mathbf{r}_1)\psi(\mathbf{r}_2)$, the energy in Eq. (6) can be written as a sum of three terms

$$E = E_0 + E_{ee} + E_{bs}, \tag{A1}$$

where E_0 is the eigenvalue of the auxiliary Schrödinger equation (4), E_{ee} is the electrostatic energy between the electrons inside the cell of radius r_s,

$$E_{ee} = \langle \psi(\mathbf{r}_1, \mathbf{r}_2) | \frac{e^2}{|\mathbf{r}_1 - \mathbf{r}_2|} | \psi(\mathbf{r}_1, \mathbf{r}_2)\rangle$$

$$= (4\pi)^2 \int_0^{r_s} dr_1 r_1 |\psi(r_1)|^2 \left\{ \int_0^{r_1} dr_2 r_2^2 |\psi(r_2)|^2 \right.$$

$$\left. + \int_{r_1}^{r_s} dr_2 r_1 r_2 |\psi(r_2)|^2 \right\}, \tag{A2}$$

and E_{bs} is a band energy correction which we will evaluate by analogy with Bardeen's derivation[40] of the effective mass valid for Bloch wave functions in the framework of the Wigner-Seitz model.[41] In this model, which is identical to our SCM, $ZV(r)$ is identified as an *effective* ionic potential, E_0 is the bottom of the band energy, and ψ is the $\mathbf{k} = 0$ Bloch wave function, solution to an equivalent to Schrödinger equation (4), which must have the symmetry of the lattice[42] and is required to satisfy the average boundary condition

$$\left. \frac{d\psi}{dr} \right|_{r_s} = 0. \tag{A3}$$

A single proton in jellium is not a periodic system and it is not immediately obvious why Eq. (A3) is the appropriate boundary condition for the SCM. The reason why it is chosen here, is that in the same way that $V(r)$ in this model is an effective potential for $r < r_s$, the boundary condition implicitly defines an *effective* potential for $r > r_s$. When the proton is completely screened at $r = r_s$, which is consistent with the other assumptions of the model, an electron will feel the same effective potential at either side of the cell boundary.

Equation (4) of the text can be solved using a series expansion

$$\psi(r) = \sum_{i=0}^{\infty} a_i r^{i+k}, \quad r \leq r_s, \tag{A4}$$

and has one solution regular at the origin, given by

$$k = 0, \quad a_1 = -Za_0, \quad a_2 = \frac{1}{3}\left(Z^2 - E_0 - \frac{3Z}{2r_s}\right)a_0,$$

$$a_3 = -\frac{1}{18}\left[Z^2 - 4\left(E_0 + \frac{3Z}{2r_s}\right)\right]a_0, \tag{A5}$$

$$a_i = \frac{-2}{i(i+1)}\left[Za_{i-1} + \left(E_0 + \frac{3Z}{2r_s}\right)a_{i-2} - \frac{Za_{i-4}}{2r_s^3}\right], \quad i \geq 4.$$

The coefficient a_0 is determined by the normalization condition

$$4\pi^2 \int_0^{r_s} dr\, r^2 |\psi(r)|^2 = 1, \tag{A6}$$

and with $k=0$, the boundary condition (A3) becomes

$$\sum_{i=0}^{\infty} (i+1)a_{i+1}r_s^i = 0, \tag{A7}$$

which gives the eigenvalue equation for E_0.

For the calculation of the effective mass, α, which enters Eq. (5), we examine the energy of the **k** Bloch state, $\psi_{\mathbf{k}} = u_{\mathbf{k}}(\mathbf{r})\exp(i\mathbf{k}\cdot\mathbf{r})$,

$$E_{\mathbf{k}} = \langle \psi_{\mathbf{k}}|(-\nabla^2/2 + \hat{V})|\psi_{\mathbf{k}}\rangle / \langle \psi_{\mathbf{k}}|\psi_{\mathbf{k}}\rangle. \tag{A8}$$

Here $u_{\mathbf{k}}$ can be expanded as $u_{\mathbf{k}} = \psi + u_1$, where ψ is the solution of Eq. (4), and u_1 of

$$-\frac{\nabla^2}{2}u_1 + ZV(r)u_1 = E_0 u_1 + i\mathbf{k}\cdot\nabla\psi. \tag{A9}$$

In Bardeen's derivation, $Z=1$, and he obtains for the effective mass

$$\alpha_B = \frac{4}{3}\pi r_s^3 |\psi(r=r_s)|^2 \left[\frac{d\ln P}{d\ln r} - 1\right]_{r=r_s}, \tag{A10}$$

where $P(r)$ is a solution of

$$\frac{d^2 P}{dr^2} - \frac{2P}{r^2} + 2[E_0 - ZV(r)]P = 0 \tag{A11}$$

with $Z=1$, which has a power series solution, $P(r) = \Sigma_{i=0}^{\infty} p_i\, r^{i+s}$, where

$$s=0, \quad p_0 = p_1 = 0, \quad p_0 = 1, \quad p_3 = -Z/2,$$

$$p_i = \frac{-2}{i^2 - i - 2}\left[Zp_{i-1} + \left(E_0 + \frac{3Z}{2r_s}\right)p_{i-2} - \frac{Z}{2r_s^3}p_{i-4}\right], \quad i \geq 4. \tag{A12}$$

However, in our case Z is a variational parameter. To account for this, we can add and subtract $ZV(r)$ in Eq. (A8). After some straightforward calculations, it can be shown that the effective mass that enters Eq. (6) is given by

$$\alpha = \alpha_B + \frac{8\pi}{3}(Z-1)\left\{\int_0^{r_s} dr[P(r) - \psi(r)r^2]^2 \right.$$

$$\left. \times [\langle\hat{V}\rangle - V(r)]\right\}, \tag{A13}$$

where α_B and P are now calculated from Eqs. (A10) and (A12), but with arbitrary variational Z, and $\langle\hat{V}\rangle = \int dr\, r^2 V(r)|\psi(r)|^2$.

Finally, we may also add a correlation energy correction to E, which within the LDA is

$$E_c = 4\pi \int_0^{r_s} dr\, r^2 |\psi(r)|^2 \varepsilon_c[|\psi(r)|^2]. \tag{A14}$$

[1] E. Wigner and H.B. Huntington, J. Chem. Phys. **3**, 764 (1935).

[2] I.F. Silvera, Rev. Mod. Phys. **52**, 393 (1980).

[3] H.K. Mao and R.J. Hemley, Rev. Mod. Phys. **66**, 671 (1994).

[4] N.W. Ashcroft, Phys. World **8**, 43 (1995).

[5] J.K. Nørskov, Phys. Rev. B **20**, 446 (1979).

[6] J.K. Nørskov, J. Chem. Phys. **90**, 7461 (1989).

[7] A. Ferraz, N.H. March, and F. Flores, J. Phys. Chem. Solids **45**, 627 (1984).

[8] O.B. Christensen, P.D. Ditlevsen, K.W. Jacobsen, P. Stoltze, O.H. Nielsen, and J.K. Nørskov, Phys. Rev. B **40**, 1993 (1989).

[9] F. Perrot and M. Rasolt, Phys. Rev. B **27**, 3273 (1983).

[10] F. Perrot, J. Phys.: Condens. Matter **6**, 431 (1994).

[11] F. Zong and D.M. Ceperley, Phys. Rev. E **58**, 5123 (1998).

[12] G. Sugiyama, L. Terray, and B.J. Alder, J. Stat. Phys. **52**, 1221 (1988).

[13] E. Zaremba, L.M. Sander, H.B. Shore, and J.H. Rose, J. Phys. F: Met. Phys. **7**, 1763 (1977).

[14] C.O. Almbladh, U. von Barth, Z.D. Popovic, and M.J. Stott, Phys. Rev. B **14**, 2250 (1976).

[15] M. Manninen, P. Hautojärvi, and R. Nieminen, Solid State Commun. **23**, 975 (1977).

[16] E.G. Brovman, Yu. Kagan, A. Kholas, and V.V. Pushkarev, JETP Lett. **18**, 160 (1973).

[17] D.M. Ceperley, *Quantum Monte Carlo Simulation of Systems at High Pressure*, in *Simple Molecular Systems at Very High Density*, edited by A. Polian, P. Loubeyre, and N. Boccara (Plenum Press, 1989).

[18] N.W. Ashcroft, J. Phys.: Condens. Matter **12**, A129 (2000).

[19] P. Hohenberg and W. Kohn, Phys. Rev. **136**, B864 (1964).

[20] W. Kohn and L.J. Sham, Phys. Rev. **140**, A1133 (1965).

[21] G. Kresse and J. Furthmüller, Phys. Rev. B **54**, 11 169 (1996).

[22] M.C. Payne, M.P. Teter, D.C. Allan, T.A. Arias, and J.D. Joannopoulos, Rev. Mod. Phys. **64**, 1045 (1992).

[23] H.J. Monkhorst and J.D. Pack, Phys. Rev. B **13**, 5188 (1976).

[24] M. Methfessel and A.T. Paxton, Phys. Rev. B **40**, 3616 (1989).

[25] D.M. Ceperley and B.J. Alder, Phys. Rev. Lett. **45**, 566 (1980).

[26] J.P. Perdew and A. Zunger, Phys. Rev. B **23**, 5048 (1981).

[27] G. Kresse and J. Hafner, J. Phys.: Condens. Matter **6**, 8245 (1994).

[28] A.M. Rappe, K.M. Rabe, E. Kaxiras, and J.D. Joannopoulos, Phys. Rev. B **41**, 1227 (1990).

[29] J. P. Perdew *Electronic Structure of Solids '91*, edited by P. Ziesche and H. Eschrig (Akademie Verlag, Berlin 1991), p. 11.

[30] J.P. Perdew, J.A. Chevary, S.H. Vosko, K.A. Jackson, M.R. Pederson, D.J. Singh, and C. Fiolhais, Phys. Rev. B **46**, 6671 (1992).

[31] M. P. Teter (private communication).

[32] Note however, that throughout this paper, in order to retain the analogy with a model where $N/2-1$ proton pairs are replaced by a uniform background, we define r_s as determined by N and not $N-2$.

[33] S. A. Bonev and N. W. Ashcroft (unpublished).

[34] The breaking of the bond is not sudden but gradual because the antibonding state is hybridized.

[35] At very high density, e.g., $r_s = 1.3$, there are no bound states at large p-p separations, and the structure is that of nearly-free electron bands, some of which are actually lowered in energy because of the attractive proton potential. The picture of immersing a hydrogen atom is then that of adding an electron at the Fermi level and pulling all bands a little down, rather than pulling a band all the way down from the Fermi level and then pushing the rest a little bit up.

[36] In an infinite system, the potential attributed to the background is a constant and the electron structure is entirely determined by the electron-electron interactions.

[37] One can improve the agreement even further by adjusting the boundary conditions a bit better, but it would be beyond the purpose of such a simplified model.

[38] We define here the screening length as the radius, r_0, around a single embedded proton such that $4\pi \int_0^{r_0} dr r^2 \delta\rho(r) = 1$, where $\delta\rho(r) = \rho(r) - 4/3\pi r_s^3$ is the induced density. At high density, where r_0 can be approximated by the inverse of the Thomas-Fermi wave vector, $r_0 \propto r_s^{1/2}$.

[39] The range may be larger; we have not attempted to establish it exactly. The p-p binding is examined by simply integrating (numerically) the Schrödinger equation with the effective *ab initio* pair potentials and for the ground state with $l = 0$ angular momentum.

[40] J. Bardeen, J. Chem. Phys. **6**, 367 (1938).

[41] D.F. Styer and N.W. Ashcroft, Phys. Rev. B **29**, 5562 (1984).

[42] The Wigner and Seitz approach is an approximate method for the calculation of the energies of the alkali metals [E. Wigner and F. Seitz, Phys. Rev. **43**, 804 (1933)].